

Machine-learning Growth at Risk^{*}

Tobias Adrian [†] Hongqi Chen[‡] Max-Sebastian Dovi[§] Ji Hyung Lee[¶]

May 2025

Abstract

We analyse growth vulnerabilities in the US using quantile partial correlation regression, a selection-based machine-learning method that achieves model selection consistency under time series. We find that downside risk is primarily driven by financial, labour-market, and housing variables, with their importance changing over time. Decomposing downside risk into its individual components, we construct sector-specific indices that predict it, while controlling for information from other sectors, thereby isolating the downside risks emanating from each sector.

^{*}The views expressed herein are those of the authors and should not be attributed to the IMF, its Executive Board, or its management.

[†]Monetary and Capital Markets Department, International Monetary Fund, tadrian@imf.org.

[‡]College of Finance and Statistics, Hunan University, hongqichen@hnu.edu.cn.

[§]African Department, International Monetary Fund, mdovi@imf.org.

[¶]Department of Economics, University of Illinois Urbana-Champaign, jihyung@illinois.edu.

1 Introduction

Analyses of downside risks to real economic activity originating in the financial sector have become a crucial part of assessing the growth outlook of economies and are routinely featured in policy reports (IMF, 2017; ECB, 2019; ESRB, 2024; IMF, 2024). Following Adrian et al. (2019), quantile regressions (QRs) have been widely adopted to assess such “growth vulnerability” – also referred to as “Growth-at-Risk” or GaR. QRs are well-suited to estimate the sensitivity of quantiles of future growth to macrofinancial conditions for two key reasons. First, QRs do not impose parametric assumptions on the distribution of growth. Second, the linearity of QRs offers clear economic interpretability, a feature that is often absent in models that feature time-varying volatility such as GARCH and certain machine-learning (ML) methods including model averaging, regression trees, random forests, and neural networks.

One key limitation of QRs is that they only allow for a small number of predictors, particularly in the tail quantiles. As a result, most GaR analyses feature a single aggregated financial conditions index (FCI) that is constructed from individual financial series. However, this approach suffers from a series of drawbacks. First, it may reduce forecasting accuracy, as aggregated FCIs may not aggregate financial information in the most relevant fashion to forecast quantiles of growth (Eguren-Martin et al., 2024).¹ Second, relying on aggregate FCIs can reduce interpretability, thereby complicating the derivation of clear policy implications. For instance, while a tightening of the National FCI (NFCI) has been shown to increase the likelihood of lower GDP growth, it remains unclear which specific components of the NFCI drive this result at any given time. Third, the inability to control for a comprehensive set of other macroeconomic predictors raises the concern that the QR coefficients on FCIs may incorrectly attribute the

¹The large literature on mean forecasting macroeconomic data has shown that relevant predictive information can be spread across several different variables (Kock et al., 2020; Bańbura et al., 2010; Kotchoni et al., 2019; Medeiros et al., 2021; Giannone et al., 2015), and recent evidence indicates that this also applies to quantile forecasting (Carriero et al., 2022; Prüser and Huber, 2024; Clark et al., 2024, 2023; Carriero et al., 2024).

effect of non-financial variables on the conditional quantiles to the FCI (Plagborg-Møller et al., 2020). Fourth, some FCIs—including the NFCI—are estimated using smoothing techniques such as Kalman filtering, which may introduce generated regressor problems as well as look-ahead bias (Amburgey and McCracken, 2023).

In this paper, we employ ML methods to simultaneously consider the effect of a large set of macrofinancial predictors on downside growth risks, and hence address the shortcomings of assessing GaR using aggregated FCIs. We furthermore show how these methods can be used to construct sector-specific indices, such as FCIs, that predict downside risk while adjusting for the influence of correlated variables in other sectors.

The first contribution of this paper is the application of ML methods to identify key financial predictors of growth vulnerabilities as measured by industrial production (IP) growth. Our paper is hence related to recent work by Prüser and Huber (2024) and Carriero et al. (2024), but our focus differs in at least three ways. First, we focus on the 0.05 quantile as this is the threshold commonly used in policy analyses, whereas Carriero et al. (2024) center their analysis on the 0.1 quantile. Second, and relatedly, we target quantiles of IP growth at the monthly frequency rather than GDP growth at the quarterly frequency because, as our simulations show, selection-based ML methods perform poorly in tail quantiles with limited observations.² Nevertheless, we show in the online appendix that our qualitative empirical results also hold when targeting GDP growth at the quarterly frequency. Third, given that these papers have already established the forecasting benefits of high-dimensional QRs, our paper focuses on the economic insights that can be gained from ML methods.

Throughout, our ML method of choice is Quantile Partial Correlation Regression (QPCR) for two reasons. First, QPCR accommodates a large number of macrofinancial predictors while preserving the key QR advantages of interpretability and robustness to ar-

²We note that the correlation between IP growth and GDP growth is 0.75 in the sample we consider, suggesting that IP growth is a good proxy for GDP growth.

bitrary distributions. Second, it offers theoretical guarantees—such as variable selection consistency—under time-series data, which provide additional reassurance when attaching interpretation to our empirical results (Chen and Lee, 2024). Moreover, we show that QPCR performs competitively against other ML methods, including non-linear models such as random forests, as well as volatility models.

Our empirical findings can be summarised as follows. We confirm the importance of financial indicators as predictors of downside growth risk, even after accounting for a comprehensive set of non-financial macroeconomic variables. We also identify additional drivers of growth vulnerabilities—namely, capacity utilisation, labour market conditions, and the housing market. Furthermore, the interpretability of QPCR enables us to validate and, importantly, quantify commonly held views regarding key predictors of downside growth risks, including the role of labour-market slack, yield curve dynamics, and credit spreads. In the online appendix, we also show that financial conditions provide information about growth tailwinds, although the relevant predictors differ from those associated with downside risks.

The second contribution of this paper is to decompose growth vulnerabilities into their individual components, and provide an easily interpretable, trackable, and comparable summary of our ML analysis in the form of sector-specific indices. Since our indices—and our FCI in particular—target a given quantile of future IP growth using a variable-selection method, they complement the targeted principal-components-based FCI proposed in Adrian et al. (2023); Eguren-Martin et al. (2024) as well as the Goldman Sachs FCI. However, our FCI offers two distinct advantages. First, it does not suffer from look-ahead bias, since it is not estimated using the entire sample but rather in a pseudo-out-of-sample fashion. Second, our index also partly addresses the concern raised in Plagborg-Møller et al. (2020) that FCIs are endogenous to broader macroeconomic developments, and hence may contain non-financial information. We achieve this by exploiting the linear structure of QPCR: incorporating a broad set of variables

ensures that the coefficients on financial variables capture their marginal effects net of the information in other variables. We note that accounting for the information contained in other sectors is especially important when creating an FCI targeted to predict a specific quantile of future growth. Indeed, the concern that an FCI may be primarily capturing information related to non-financial variables is heightened when it is constructed by targeting particular quantiles of a non-financial variable such as IP growth. Our FCI hence also bears some similarity to the Adjusted NFCI, which controls for non-financial macroeconomic variables in a similar way, but does not target specific quantiles (Brave and Kelley, 2017).

Our financial, labour-market, and housing indices are strongly correlated with established benchmarks in these respective sectors, while being at most weakly correlated with indicators from other sectors, which enables them to isolate each sector’s predictive information. By contrast, the NFCI shows significant correlations with standard labour-market and housing measures, which suggests that it also incorporates non-financial signals. Taken together, these findings highlight the value of constructing dedicated, sector-specific indices using our proposed approach.

The rest of this paper is organised as follows. Section 2 provides an overview of QPCR and the other approaches we use for comparison. Section 3 provides simulation evidence in favour of evaluating GaR at the monthly frequency using IP growth. Section 4 presents the results. The last section concludes.

2 Model and methodology

We study the predictive relationship between the scalar sequence of IP Growth rates, $\{Y_{t+1}\}_{t=1}^T$, and a sequence of stationary β -mixing predictors $\{X_t\}_{t=1}^T$, where $X_t = (X_{t,1}, \dots, X_{t,p})' \in \mathbb{R}^p$, and p can be larger than T . Throughout, we assume that

$\{Y_{t+1}, X_t\}_{t=1}^T$ and X_{T+1} are observed.

For all models except for the GARCH model discussed below, we select covariates to predict the conditional quantile $\tau \in (0, 1)$ of Y_{t+1} given X_t , which we model as

$$Q_{Y_{t+1}}(\tau|X_t) = X_t' \beta_\tau.$$

For simplicity, we suppress the τ subscript in β_τ , and use j instead of t in X_j to represent a particular covariate, denoted as $(X_{1,j}, \dots, X_{T,j})' \in \mathbb{R}^T$ for $j = 1, \dots, p$. Following standard notation, the quantile loss function is defined as $\rho_\tau(u) = u(\tau - 1(u < 0))$, and its subgradient is given by $\psi_\tau(u) = \tau - 1(u < 0)$.

2.1 Quantile Partial Correlation Regression

In order to outline QPCR as used in Ma et al. (2017); Chen and Lee (2024), we introduce the following notation and definitions. Let $S \subseteq \{1, \dots, p\}$ denote a generic index set of the covariate vector X_t , and $X_{t,S}$ denote the elements of X_t indexed by S . We define the population quantile partial correlation (QPC) at the τ -th quantile level for random variables $\{Y_{t+1}, X_{t,j}, X_{t,S}\}$ as:

$$\begin{aligned} qpcor_\tau(Y_{t+1}, X_{t,j}|X_{t,S}) &= \frac{\text{cov}(\psi_\tau(Y_{t+1} - X_{t,S}'\alpha_S^0), X_{t,j} - X_{t,S}'\theta_{j,S}^0)}{\sqrt{\text{var}(\psi_\tau(Y_{t+1} - X_{t,S}'\alpha_S^0)) \text{var}(X_{t,j} - X_{t,S}'\theta_{j,S}^0)}} \\ &= \frac{E[\psi_\tau(Y_{t+1} - X_{t,S}'\alpha_S^0)(X_{t,j} - X_{t,S}'\theta_{j,S}^0)]}{\sqrt{\tau(1-\tau)\sigma_{t,j}^2}}, \end{aligned}$$

where $\alpha_S^0 = \arg \min_{\alpha_S} E(\rho_\tau(Y_{t+1} - X_{t,S}'\alpha_S))$, $\theta_{j,S}^0 = \arg \min_{\theta_{j,S}} E((X_{t,j} - X_{t,S}'\theta_{j,S})^2)$, and $\sigma_{t,j}^2 = \text{var}(X_{t,j} - X_{t,S}'\theta_{j,S}^0)$. Its sample analogue, denoted \widehat{qpcor}_τ , is given by

$$\widehat{qpcor}_\tau(Y_{t+1}, X_{t,j}|X_{t,S}) = \frac{\frac{1}{T} \sum_{t=1}^T (\psi_\tau(Y_{t+1} - X_{t,S}'\hat{\alpha}_S)(X_{t,j} - X_{t,S}'\hat{\theta}_{j,S}))}{\sqrt{\tau(1-\tau)\hat{\sigma}_{t,j}^2}},$$

where $\hat{\alpha}_S = \arg \min_{\alpha_S} \frac{1}{T} \sum_{t=1}^T \rho_\tau(Y_{t+1} - X'_{t,S} \alpha_S)$ is the QR estimator of the quantile regression of Y_{t+1} on $X_{t,S}$, $\hat{\theta}_{j,S} = \arg \min_{\theta_{j,S}} \frac{1}{T} \sum_{t=1}^T (X_{t,j} - X'_{t,S} \theta_{j,S})^2$ is the OLS estimator of the projection of $X_{t,j}$ on $X_{t,S}$, and $\hat{\sigma}_{t,j}^2 = \frac{1}{T} \sum_{t=1}^T (X_{t,j} - X'_{t,S} \hat{\theta}_{j,S})^2$ is the variance estimator of the residual in the projection of $X_{t,j}$ on $X_{t,S}$. Finally, let $\hat{\varrho}_{j,k}$ be the sample correlation coefficient between X_j and X_k , and for every $j = 1, \dots, p$, define $\hat{j}(m) \neq j$ as the index of the variable such that $|\hat{\varrho}_{j,\hat{j}(m)}|$ is the m -th largest value in the set $\{|\hat{\varrho}_{j,l}|\}_{l=1, l \neq j}^p$, as well as the confounding set

$$\begin{aligned} S_j^\nu(m) &:= S_j^\nu(\{X_t\}_{t=1}^T, m) \\ &= \left\{ k \in \{1, \dots, p\} : k \neq j \text{ and } |\hat{\varrho}_{j,k}| \geq |\hat{\varrho}_{j,\hat{j}(m)}| \right\}. \end{aligned}$$

With this notation and definitions in place, Algorithm 1 describes QPCR. Intuitively, the algorithm iteratively selects the variables that are most predictive of the τ -th quantile of the dependent variable, conditional on the previously selected variable as well as the variables most highly correlated with it. We note that QPCR offers a series of advantages over competing ML methods. First, as shown in Chen and Lee (2024) under suitable assumptions that allow for time series, QPCR is theoretically guaranteed to eventually select all relevant predictors even if the number of predictors outstrips the number of observations ($p > T$). Second, QPCR helps mitigate the problem of correlated predictors that can affect many popular ML methods such as the LASSO (see, e.g., Sun and Medeiros (2024)), since the inclusion of the conditioning set ensures that candidate predictors that are highly correlated with previously selected predictors are not selected.

The QPCR algorithm depends on hyperparameters, which we set as follows. The confounding set is updated $d^* = \left\lfloor \frac{T}{\log T} \right\rfloor^{\frac{1}{2}}$ times, and, following Ma et al. (2017), the total number of iterations is $D_{max} = \left\lfloor \frac{T}{\log T} \right\rfloor$. The size of the confounding set is controlled by the parameters m_d for $d = 1, \dots, d^*$, which we set equal to $m_d = \left\lfloor \frac{T}{\log T} \right\rfloor^{\frac{1}{2}}$. We note that our choice of D^* in Algorithm 1, which determines the number of predictors, cor-

responds to choosing the number of predictors that minimises the extended Bayesian information criterion (EBIC), and we choose $C = 1$.

Algorithm 1 Quantile Partial Correlation Regression

- 1: Choose the quantile level $\tau \in (0, 1)$, the number of updates to the confounding set $d^* \in \mathbb{N}$, the maximum number of predictors to be added to the confounding set at each update $\{m_j \in \mathbb{N}\}_{j=1}^{d^*}$, the maximum number of iterations $D_{\max} \in \mathbb{N}$, and the EBIC constant $C \in \mathbb{R}$
- 2: Initialize active set $S_1 = \emptyset$ and $S_1^\nu(m_1) = \emptyset$
- 3: **for** $d = 1$ to D_{\max} **do**
- 4: Set $\bar{S}_d = S_d \cup S_d^\nu(m_{\bar{d}})$ for $\bar{d} = \min(d, d^*)$
- 5: Select covariate index

$$j^* = \arg \max_{j \notin \bar{S}_d} |\widehat{qpcor}_\tau(Y_{t+1}, X_{t,j} \mid X_{t,\bar{S}_d})|$$

- 6: Update $S_{d+1} = S_d \cup \{j^*\}$
- 7: **end for**
- 8: Calculate

$$D^* = \arg \min_{D \in \mathbb{N}, D \leq D_{\max}} \log \left(\frac{1}{T} \sum_{t=1}^T \rho_\tau \left(Y_t - X'_{t,S_D} \hat{\beta}_{S_D}^{QPCR} \right) \right) + C \frac{\log T \log D}{T},$$

and

$$\hat{\beta}_{S_D}^{QPCR} = \arg \min_{\beta_{S_D} \in \mathbb{R}^{|S_D|}} \frac{1}{T} \sum_{t=1}^T \rho_\tau(Y_{t+1} - X'_{t,S_D} \beta_{S_D})$$

- 9: Calculate the estimated Quantile Partial Correlation Regression coefficient as the vector $\hat{\beta}^{QPCR} \in \mathbb{R}^p$ where $\hat{\beta}_j^{QPCR} = \hat{\beta}_{S_{D^*},j}^{QPCR}$ if $j \in S_{D^*}$ and $\hat{\beta}_j^{QPCR} = 0$ otherwise
 - 10: Calculate the conditional quantiles $Q_{Y_{t+1}}^{QPCR}(\tau | X_t) = X'_t \hat{\beta}^{QPCR}$ for $t = 1, \dots, T + 1$.
-

2.2 Other methods

This section presents additional methods used in our forecasting exercise, including state-of-the-art quantile ML forecasting techniques and standard volatility models. We consider three linear penalization-based quantile ML methods: the l_1 -penalized LASSO (l_1 -QR) following Belloni and Chernozhukov (2011); Tibshirani (1996), the smoothly-clipped absolute deviation (SCAD) penalty from Fan and Li (2001), and the minimax concave penalty (MCP) proposed by Zhang (2010). While these techniques lack theoretical guarantees for time series data, they are widely applied in high-dimensional regression models. We also include Quantile Random Forests (QRFs), a nonlinear ML approach that outperforms Quantile Neural Nets in our forecasting exercises,³ and to the best of our knowledge has not yet been considered in the GaR literature (see Lenza et al. (2023) for an application to inflation forecasting). Finally, we consider a standard GARCH model as employed in Brownlees and Souza (2021).

2.2.1 Penalized quantile regression

For all three penalized QR methods, the estimator takes the form

$$\hat{\beta}^i = \arg \min_{\beta} \frac{1}{T} \sum_{t=1}^T \rho_{\tau} \left(Y_{t+1} - X'_t \beta \right) + \sum_{j=1}^p q_{\lambda,a}(\beta_j),$$

and the conditional quantile takes the form $Q_{Y_{t+1}}^i(\tau|X_t) = X'_t \hat{\beta}^i$ for $t = 1, \dots, T+1$, where $q_{\lambda,a}(\beta_j)$ is a penalty function depending on scalars $\lambda \geq 0$ and $a \geq 0$, and $i \in \{l_1\text{-QR}, \text{SCAD}, \text{MCP}\}$.

³In particular, using QNNs with 3 to 24 hidden nodes and ReLU activation, we found that the forecasting performance of QNNs is worse than that of QPCR and QRFs. Moreover, QNNs suffer from several limitations, including a lack of interpretability, and a large number of hyperparameters that require tuning. For these reasons, we do not include QNNs in the main text.

For l_1 -QR, the penalty function is

$$q_{\lambda,a}(\beta_j) = \lambda |\beta_j|.$$

The SCAD method employs the penalty function $q_{\lambda,a}(\beta)$, whose derivative is given by:

$$q'_{\lambda,a}(\beta) = \lambda \left[\mathbf{1}(\beta \leq \lambda) + \frac{\max\{a\lambda - \beta, 0\}}{(a-1)\lambda} \mathbf{1}(\beta > \lambda) \right],$$

where $a > 2$ is a tuning parameter controlling the nonconvexity of the penalty. The MCP method employs the penalty function $q_{\lambda,a}(\beta)$, with its derivative defined as:

$$q'_{\lambda,a}(\beta) = \begin{cases} \operatorname{sgn}(\beta) \left(\lambda - \frac{|\beta|}{a} \right) & \text{if } |\beta| \leq a\lambda \\ 0 & \text{otherwise} \end{cases}$$

where $a > 1$ is a tuning parameter that controls the decay speed of the penalty. Following standard practice in the literature, we use the 5-fold cross-validation criterion to choose the optimal λ and a . We note that contrarily to QPCR, these methods do not come with any theoretical guarantees under time series.

2.2.2 Quantile random forests

In this subsection, we briefly review the QRF methods proposed by Meinshausen (2006) and Athey et al. (2019), which we term QRFM and QRFATW, respectively. Algorithm 2 provides the implementation details. Intuitively, the key idea is to construct an ensemble of decision trees that assign weights to past observations based on their similarity to the vector of covariates used in the prediction step, and then estimate the conditional quantile via a weighted quantile loss function. QRFM and QRFATW follow a similar tree-based structure, but differ in their splitting criteria: QRFM seeks to maximise the difference in conditional means between child nodes, while QRFATW maximises the

differences in empirical conditional quantiles.

We set the number of trees to $B = 2000$ and use a minimum terminal node size of $m = 5$ as the stopping criterion. At each split, a random subset of $\lfloor p^{\frac{1}{2}} \rfloor + 20$ covariates is considered for selecting the splits (i.e., $J = 20$).

Algorithm 2: *Quantile Random Forests (QRFM and QRFATW)*

- 1: Choose the quantile level $\tau \in (0, 1)$, the number of trees $B \in \mathbb{N}$, minimum leaf size $m \in \mathbb{N}$, the constant to be added to feature subsample size $J \in \mathbb{N}$, and the conditioning predictors $x \in \mathbb{R}^p$
- 2: **for** $b = 1$ to B **do**
- 3: Draw a sample $\mathcal{D}_b = \{(Y_{t+1}^*, X_t^*)\}_{t=1}^{\lfloor T/2 \rfloor}$ without replacement from $\{(Y_{t+1}, X_t)\}_{t=1}^T$
- 4: Randomly split \mathcal{D}_b into two samples of equal size, $\mathcal{D}_b^{\text{tree}}$ and $\mathcal{D}_b^{\text{weights}}$
- 5: Initialize queue: $\text{Queue} \leftarrow \{(\mathcal{D}_b^{\text{tree}}, \text{Path} = \emptyset)\}$, $k = 0$
- 6: **while** Queue is not empty **do**
- 7: Pop $(\mathcal{D}_{b,\text{leaf}}, \text{Path})$ from Queue⁴
- 8: **if** $|\mathcal{D}_{b,\text{leaf}}| \leq m$ **then**
- 9: Store $\mathcal{W}_{b,k} := \{x \in \mathbb{R}^p : x \text{ satisfies all conditions in ordered Path}\}$
- 10: Set $k = k + 1$
- 11: **else**
- 12: Select $\mathcal{S} \subseteq \{1, \dots, p\}$ uniformly at random with $|\mathcal{S}| = \lfloor \sqrt{p} \rfloor + J$
- 13: For each $j \in \mathcal{S}$ and split value s , define:

$$\mathcal{L}_{j,s} = \{(Y_{t+1}^*, X_t^*) \in \mathcal{D}_{b,\text{leaf}} : X_{t,j}^* \leq s\}$$

$$\mathcal{R}_{j,s} = \{(Y_{t+1}^*, X_t^*) \in \mathcal{D}_{b,\text{leaf}} : X_{t,j}^* > s\}$$

⁴That is, take the last element from **Queue**, $(\mathcal{D}_{b,\text{leaf}}, \text{Path})$, and remove it from **Queue**

14: **if** QRFM (mean-based split) **then**

$$j^*, s^* = \arg \max_{j \in \mathcal{S}, s \in \mathbb{R}} \sum_{\mathcal{C} \in \{\mathcal{L}_{j,s}, \mathcal{R}_{j,s}\}} |\hat{Y}(\mathcal{C}) - \hat{Y}(\mathcal{D}_{b,\text{leaf}})|$$

$$\hat{Y}(\mathcal{K}) = \frac{1}{|\mathcal{K}|} \sum_{(Y_{t+1}^*, X_t^*) \in \mathcal{K}} Y_{t+1}^* \quad \text{for } \mathcal{K} \in \{\mathcal{L}_{j,s}, \mathcal{R}_{j,s}, \mathcal{D}_{b,\text{leaf}}\}$$

15: **else if** QRFATW (quantile-based split) **then**

$$j^*, s^* = \arg \max_{j \in \mathcal{S}, s \in \mathbb{R}} \sum_{\mathcal{C} \in \{\mathcal{L}_{j,s}, \mathcal{R}_{j,s}\}} |\hat{Q}(\mathcal{C}, \tau) - \hat{Q}(\mathcal{D}_{b,\text{leaf}}, \tau)|$$

$$\hat{Q}(\mathcal{K}, \tau) = \inf \left\{ y \in \mathbb{R} : \frac{1}{|\mathcal{K}|} \sum_{(Y_{t+1}^*, X_t^*) \in \mathcal{K}} \mathbf{1}(Y_{t+1}^* \leq y) \geq \tau \right\}$$

for $\mathcal{K} \in \{\mathcal{L}_{j,s}, \mathcal{R}_{j,s}, \mathcal{D}_{b,\text{leaf}}\}$

16: **end if**

17: Append $(\mathcal{L}_{j^*, s^*}, \text{Path} \leftarrow \text{Path} \text{ appended with } (j^*, s^*, \text{left}) \text{ to Queue}$

18: Append $(\mathcal{R}_{j^*, s^*}, \text{Path} \leftarrow \text{Path} \text{ appended with } (j^*, s^*, \text{right}) \text{ to Queue}$

19: **end if**

20: **end while**

21: Save the number of leaves in tree b , $l_b = k$

22: **end for**

23: Calculate $\{\mathcal{W}_{b,k(x)}\}_{b=1}^B$ such that $x \in \mathcal{W}_{b,k(x)}$ for all $b = 1, \dots, B$

24: Compute weights

$$w_t(x) = \frac{1}{B} \sum_{b=1}^B \left| \left\{ (Y_{t+1}^*, X_t^*) \in \mathcal{D}_b^{\text{weights}} : X_t^* \in \mathcal{W}_{b,k(x)} \right\} \right|$$

25: Return

$$\hat{Q}_{Y_{t+1}}(\tau \mid x) = \arg \min_{q \in \mathbb{R}} \left\| \sum_{t=1}^T w_t(x) (\tau - \mathbf{1}(Y_{t+1} \leq q)) \right\|_2$$

2.2.3 GARCH

In addition to ML quantile regression methods, we also consider a standard GARCH approach as in Brownlees and Souza (2021),

$$Y_{t+1} = \mu_{t+1|t} + \sigma_{t+1|t} Z_{t+1},$$

where $Z_{t+1} \stackrel{i.i.d.}{\sim} \mathcal{D}(0, 1)$, and $\mathcal{D}(0, 1)$ is a location-scale distribution with mean 0 and variance 1. $\mu_{t+1|t}$ and $\sigma_{t+1|t}$ are the mean and standard deviation of Y_{t+1} conditional on information available at time t . The conditional quantile can then be expressed as

$$Q_{Y_{t+1}}(\tau | \mathcal{F}_t) = \mu_{t+1|t} + \sigma_{t+1|t} F_{\mathcal{D}}^{-1}(\tau),$$

where $F_{\mathcal{D}}^{-1}(\cdot)$ is the inverse cumulative density function of the distribution $\mathcal{D}(0, 1)$, and $\{\mathcal{F}_t\}_{t \geq 0}$ is the natural filtration (information set) at time t . We follow the bootstrapped simulation approach suggested in Brownlees and Souza (2021, Algorithm 1) to determine $F_{\mathcal{D}}^{-1}(\tau)$. We formulate an AR(1) model for the conditional mean, $\mu_{t+1|t} = \phi_0 + \phi_1 Y_t$, and a GARCH(1,1) model for the conditional variance, $\sigma_{t+1|t}^2 = \omega + \alpha (Y_t - \mu_{t|t-1})^2 + \gamma \sigma_{t|t-1}^2$.

3 Simulations

We conduct stylised simulations to show that large samples are essential for correctly identifying relevant predictors in tail quantiles, justifying our focus on assessing growth vulnerabilities at the monthly frequency using IP Growth. To highlight that this issue does not stem from an especially unfavourable data-generating process (DGP), we employ a very simple DGP that is not necessarily intended to represent GaR dynamics.

We generate predictors as the absolute values of independent draws from a multivari-

ate Normal distribution to ensure non-negativity in the location-scale linear quantile regression formulation, and, for simplicity, we set $X_{t,j} \stackrel{i.i.d.}{\sim} |\mathcal{N}(0, 1)|$ for $t = 1, \dots, T$ and $j = 1, \dots, p$. We model the response variable y_{t+1} by a location-scale framework

$$Y_{t+1} = X_t' \alpha_t + (X_t' \beta_t) \epsilon_t,$$

where α_t and β_t are p -dimensional column vectors with entries $\alpha_{t,j}, \beta_{t,j}$, and $\epsilon_t \stackrel{i.i.d.}{\sim} \mathcal{N}(0, 1)$. Consequently, the conditional linear quantile function for Y_{t+1} is

$$Q_{Y_{t+1}}(\tau|X_t) = X_t'(\alpha_t + \beta_t \Phi^{-1}(\tau)).$$

We consider a fixed sparse, a time-varying sparse, and a dense setup. Under the fixed sparse setup, for all $t = 1, \dots, T$, $\beta_{t,j} = 1$, $\alpha_{t,j} = -1$ for $j = 1, \dots, s$, and $\beta_{t,j} = \alpha_{t,j} = 0$ otherwise. For the time-varying sparse setup, $\beta_{t,j} = 1$, $\alpha_{t,j} = -1$ for $j = 1, \dots, s$, $t = 1, \dots, \lfloor T/2 \rfloor$, $\beta_{t,j} = 0.5$, $\alpha_{t,j} = -1$ for $j = 1, \dots, s$, $t = \lfloor T/2 \rfloor + 1, \dots, T$, and $\beta_{t,j} = \alpha_{t,j} = 0$ otherwise. For the dense setup, for all $t = 1, \dots, T$, $\beta_{t,j} = 1$, $\alpha_{t,j} = -1$ for $j = 1, \dots, s$, and $\beta_{t,j} = \alpha_{t,j} = 1/p$ otherwise. For all DGPs, we denote the predictors indexed by $j = 1, \dots, s$ as the ‘relevant predictors’. Thus, all setups feature s relevant predictors, but differ in terms of the informativeness of the other predictors, as well as the stability of the coefficients over time.

For all setups, we set $s = 5$ and $\tau = 0.05$. To illustrate that large samples are needed to correctly identify relevant predictors in tail quantiles, we consider values of T and p that roughly match the FRED database at the monthly and quarterly frequency, i.e., $T = 500, p = 110$ and $T = 100, p = 220$, respectively. For each of the selection-based ML methods presented in Section 2, we report the selection frequency of the relevant predictors, as well as the average number of times non-relevant predictors are selected (‘false selections’) across 1000 simulations.

Table 1 presents the simulation results. For $T = 500, p = 110$, all selection-based

Table 1: Simulation results

Setup	Method	$T = 500, p = 110$						$T = 100, p = 220$					
		X_1	X_2	X_3	X_4	X_5	Avg. false	X_1	X_2	X_3	X_4	X_5	Avg. false
Fixed sparse	QPCR	0.90	0.88	0.90	0.90	0.89	1.17	0.10	0.10	0.10	0.10	0.12	3.47
	l_1 -QR	0.97	0.97	0.97	0.97	0.97	15.12	0.14	0.12	0.14	0.12	0.15	2.65
	SCAD	0.95	0.95	0.95	0.94	0.95	7.32	0.14	0.13	0.14	0.14	0.15	2.97
	MCP	0.95	0.95	0.95	0.94	0.95	7.54	0.15	0.15	0.16	0.13	0.16	3.09
Time-varying sparse	QPCR	0.88	0.86	0.86	0.86	0.86	1.42	0.10	0.12	0.10	0.12	0.11	3.61
	l_1 -QR	0.94	0.94	0.94	0.94	0.94	14.57	0.14	0.13	0.14	0.12	0.15	2.92
	SCAD	0.93	0.92	0.91	0.92	0.92	7.57	0.14	0.13	0.14	0.14	0.16	3.05
	MCP	0.92	0.92	0.91	0.91	0.92	7.87	0.14	0.15	0.15	0.13	0.16	3.20
Dense	QPCR	0.81	0.81	0.81	0.80	0.79	2.17	0.09	0.08	0.07	0.09	0.08	3.61
	l_1 -QR	0.91	0.93	0.92	0.91	0.91	13.95	0.12	0.11	0.11	0.10	0.13	2.65
	SCAD	0.86	0.87	0.86	0.85	0.86	7.29	0.13	0.11	0.13	0.11	0.14	2.96
	MCP	0.86	0.86	0.84	0.83	0.86	7.49	0.12	0.11	0.12	0.10	0.14	2.95

Note. Selection frequencies for the five relevant predictors (X_1 to X_5) and average false selections for different selection-based ML methods and simulation setups over 1000 simulations. QPCR denotes to the quantile partial correlation regression. l_1 -QR, SCAD, and MCP refer to penalized quantile regressions using the l_1 penalty, smooth-clipped absolute deviation penalty, and minimax concave penalty, respectively.

methods select the relevant predictors with high frequency, and QPCR has the lowest average false selection rate. In contrast, for $T = 100, p = 220$, all selection-based methods fail to reliably select the relevant predictors, and the average false selection rate is similarly high across all methods. Motivated by these findings, our main empirical analysis focuses on monthly IP-growth (420 observations) rather than quarterly GDP-growth (only 111 observations). Nevertheless, in the online appendix, we also report our estimation results using GDP growth as the dependent variable.

4 Empirical results

Throughout this section, we consider a rolling-window pseudo-out-of-sample forecasting exercise for $\tau = 0.05$ on monthly data from the Fred-MD. Our sample spans January 1971 through October 2024, and we transform the data as recommended in McCracken and Ng (2020). Each estimation window contains 420 observations and 111 predictors. Beginning in January 2006, we produce one-step-ahead forecasts for each month up

to October 2024, yielding 225 out-of-sample predictions. In Section 4.1, we compare the forecasting performance of QPCR to the other methods described in Section 2, showing that QPCR performs competitively. In Section 4.2 we analyse the drivers of downside risk over time. In Section 4.3 we decompose growth vulnerabilities into their individual components, and construct sector-specific indices. The online appendix contains analogous results for upside risks, i.e., $\tau = 0.95$.

4.1 Forecasting performance

We evaluate the forecasting performance using the mean quantile prediction error (MPE) defined as

$$MPE = \frac{1}{T_{out}} \sum_{t=1}^{T_{out}} \rho_{\tau}(y_t - \hat{y}_{t,\tau}),$$

where T_{out} is the total number of out-of-sample forecasting period, y_t is the IP growth rate one period after the last observation in the estimation sample, and $\hat{y}_{t,\tau}$ is its predicted conditional τ -quantile. We also evaluate standard Diebold-Mariano tests comparing QPCR to the other methods outlined in Section 2, although we note that they may not have the usual interpretation when ML methods lack necessary theoretical guarantees.

The MPEs and DM statistics reported in Table 2 show that QPCR performs favorably compared to other ML methods, including non-linear QRF. We hence conclude that QPCR is highly suited to analysing GaR, since it comes with theoretical guarantees under time-series data, provides interpretable results by selecting relevant predictors, and performs competitively against other linear and non-linear ML and volatility models.

Table 2: Forecasting performance, $\tau = 0.05$

Method	MPE ($\times 10^{-3}$)	DM-Statistics (QPCR/Others)
QPCR	1.462	–
l_1 -QR	1.692	-1.378
SCAD	1.769	-2.017
MCP	1.759	-1.855
QRFATW	1.480	-0.154
QRFM	1.449	0.114
GARCH	1.599	-1.445

Note. Negative DM values indicate that QPCR outperforms the corresponding method. Under appropriate regularity conditions, DM test statistics are asymptotically normally distributed and the usual critical values of ± 1.96 apply. QPCR denotes to the quantile partial correlation regression. l_1 -QR, SCAD, and MCP refer to penalized quantile regressions using the l_1 penalty, smooth-clipped absolute deviation penalty, and minimax concave penalty, respectively. QRFATW and QRFM represent the quantile random forests proposed by Athey et al. (2019) and Meinshausen (2006), respectively.

4.2 Drivers of downside risk

To avoid muddying our discussion by predictors that are only sporadically selected, we focus on those predictors that are selected in at least twelve consecutive months. The resulting heat map of these ‘systematically selected’ predictors for $\tau = 0.05$ is shown in Figure 1. We find that the main drivers of downside risk (after controlling for the lag of industrial production) to GDP can be categorised into just four groups: capacity utilisation (CUMFNS), labour-market indicators (UNRATE, CLAIMSx, PAYEMS, USGOOD, SVPRD, AWHMAN), housing-related indicators (HOUST, HOUSTS, PERMIT), and financial indicators (CP3Mx, COMPAPFFx, TB3SMFFM, TB6SMFFM, AAFM, VIXCLSx).

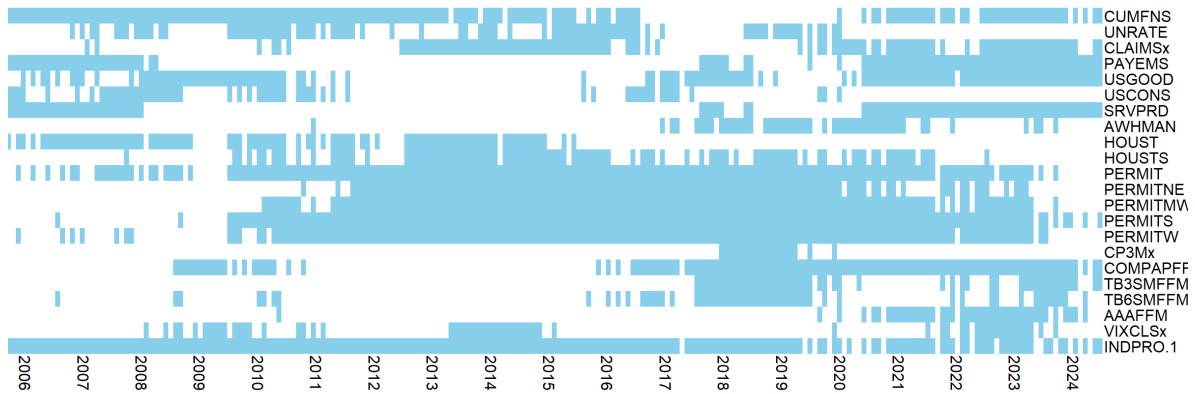


Figure 1: Selected variables for $\tau = 0.05$

Note. Variables selected for at least 12 consecutive months. Each row represents a selected variable, and blue cells indicate periods of selection. CUMFNS: capacity utilisation; UNRATE: unemployment rate; CLAIMSx: initial claims; PAYEMS: total nonfarm employees; USGOOD: goods-producing employees; USCONS: construction employees; SRVPRD: service-producing employees; AWHMAN: average weekly hours (manufacturing); HOUST: housing starts; HOUSTS: housing starts (south); PERMIT: new private housing permits; PERMITNE: new private housing permits (northeast); PERMITMW: new private housing permits (midwest); PERMITS: new private housing permits (south); CP3Mx: three-month AA financial commercial paper rate; COMPAPFFx: three-month commercial paper rate minus Federal Funds rate; TB3SMFFM: three-month Treasury rate minus Federal Funds rate; TB6SMFFM: six-month Treasury rate minus Federal Funds rate; AAAFFM: Moody's Aaa corporate bond rate minus Federal Funds rate; VIXCLS: VIX; INDPRO.1: lag of industrial production.

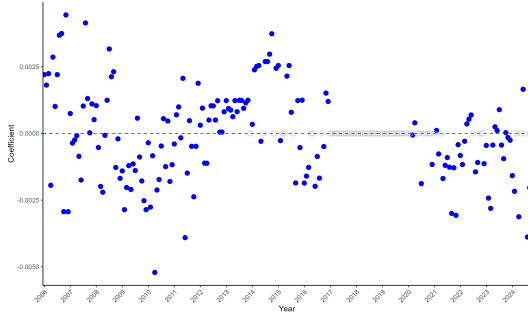
Figure 1 also shows how the predictors of downside risk have changed over time. Housing and labour-market indicators are consistently selected. Financial variables exhibit time-varying importance, with notable spikes in selection during periods of financial stress such as the Global Financial Crisis (GFC) and the Covid-19 pandemic. For instance, the commercial paper spread and the VIX are selected consistently during and surrounding the great financial crisis. Moreover, at the end of the Covid-19 pandemic and during the subsequent inflation surge, spreads and the VIX are also consistently selected.

The commercial paper spread (COMPAPFFx) is consistently selected starting in 2016, suggesting that changes in short-term financing conditions of companies have become an important transmission channel of monetary policy.

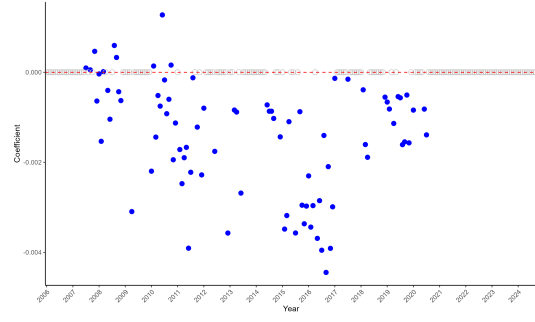
One of the benefits of QPCR over other ML methods is the interpretability of its results. Figure 2 shows coefficient estimates over time of some of the selected variables in the groups described above: CUMFNS (capacity utilisation), UNRATE (unemployment rate), CLAIMsx (initial claims), COMPAPFFx (three-month commercial paper minus the Federal Funds rate), HOUST (housing starts), and TB6SMFFM (six-month Treasury rate minus the Federal Funds rate). The first panel shows that the sign of the effect of capacity utilisation on growth vulnerability varies substantially over time, making it difficult to attach economic interpretation to this coefficient.

By contrast, the second and third panels show that increases in labour market slack—as measured by higher unemployment or initial claims—consistently worsen growth vulnerabilities. This is consistent with the view that supply shocks originating in the labour market increase recession risks. The fourth panel shows that that housing starts increased growth vulnerabilities, but only in the period surrounding the great financial crisis. Since approximately 2016, this predictor ceases to be informative about growth vulnerabilities, potentially reflecting improved macroprudential regulation. The fifth panel shows that increases in the commercial paper spread worsen growth vulnerabilities. This is consistent with the view that higher costs of firm financing—potentially reflecting heightened credit or liquidity risk—can translate into weaker investment and hence higher recession risk (see also Gilchrist and Zakrajšek (2012); Gertler and Lown (1999)). The final panel shows that a widening spread between the six-month Treasury-bill rate and the Federal Funds rate is linked to lower growth vulnerabilities. This result is consistent with the view that yield-curve steepenings reflect expectations of economic recovery arising from anticipated monetary policy normalisation (see, e.g., (Estrella and Mishkin, 1998)).

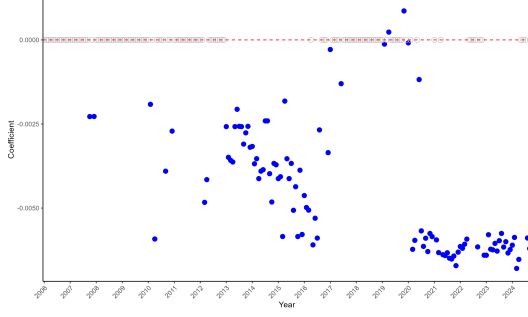
We hence conclude that the main predictors identified by QPCR are consistent with commonly held heuristics to assess recession risks. Importantly, however, the results further quantify these heuristics while controlling for the effect of all other predictors. For instance, we find that after controlling for all other variables, an increase in the unemployment rate of one standard deviation decreases the predicted lower-tail quantile ($\tau = 0.05$) of industrial production growth by up to half a percentage point. Similarly, after controlling for all other variables, we find that during the most recent hiking cycle, a one standard deviation increase in the commercial paper spread decreased the predicted lower-tail quantile ($\tau = 0.05$) of industrial production growth by one percentage point. Such quantification is particularly valuable for policymakers, as it clearly identifies which factors drive recession risk and measures their potential impact.



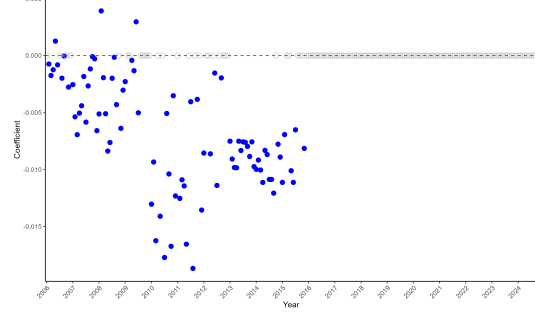
(a) CUMFNS



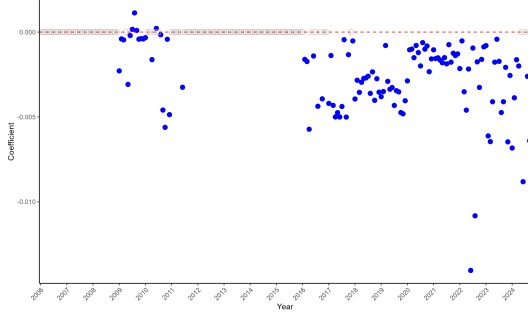
(b) UNRATE



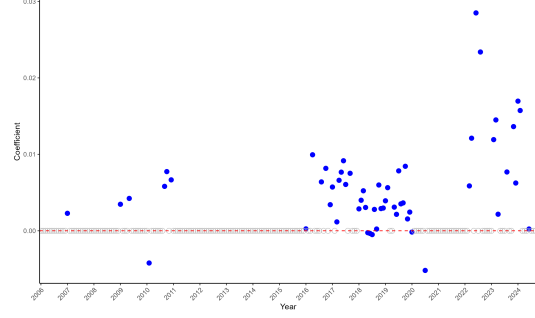
(c) CLAIMSx



(d) HOUST



(e) COMPAPFFx



(f) TB6SMFFM

Figure 2: Coefficients of selected variables for $\tau = 0.05$ over time.

Note. Solid blue dots indicate periods of selection and show the corresponding value of the estimate. Hollow dots represent periods in which the variable was not selected. See Figure 1 for definitions of the acronyms.

4.3 Growth at Risk decomposition and targeted indices

An advantage of QPCR is that the predicted growth vulnerabilities can easily be decomposed into their underlying drivers. Letting $\mathcal{G} \subseteq \{1, \dots, p\}$ denote the indices corresponding to a particular set of variables (e.g., financial variables), we can write the total contribution of the predictors indexed in \mathcal{G} to one-step-ahead growth vulnerabilities based on the sample $\{Y_{t+1}, X_t\}_{t=1}^T$ and the conditioning predictor X_{T+1} as

$$\hat{Q}_{Y_{T+2}}^{QPCR, \mathcal{G}}(\tau | X_{\mathcal{G}, T+1}) = \sum_{j \in \mathcal{G}} \hat{\beta}_j^{QPCR} X_{T+1, j}.$$

We note that if $\mathcal{G}_1, \dots, \mathcal{G}_n$ form a partition of $\{1, \dots, p\}$, the quantile of Y_{T+2} conditional on X_{T+1} , i.e., GaR, can be expressed as $\hat{Q}_{Y_{T+2}}^{QPCR}(\tau | X_{T+1}) = \sum_{i=1}^n \hat{Q}_{Y_{T+2}}^{QPCR, \mathcal{G}_i}(\tau | X_{\mathcal{G}_i, T+1})$.

Figure 3 shows the GaR decomposition for $\tau = 0.05$, with contributions aggregated across Fred-MD group labels, as well as the lag of IP growth and a constant. During the GFC, the labour, housing, and stock markets were key sources of vulnerability. In the post-GFC period and leading up to the Covid-19 pandemic, vulnerabilities declined, with the constant term emerging as the main contributor to downside risk. During the Covid-19 pandemic, the labour market became the dominant driver of downside risk.



Figure 3: Decomposition of GaR into Fred-MD groups, $\tau = 0.05$.

Note. Each stacked bar represents the contribution to the predicted conditional quantile of a specific group of indicators, $\hat{Q}_{Y_{T+2}}^{QPCR, \mathcal{G}_i}(\tau | X_{\mathcal{G}_i, T+1})$, where \mathcal{G}_i are the group labels in FRED-MD, as well as the lag of IP, and the constant. The black solid line shows the predicted conditional quantile, $\hat{Q}_{Y_{T+2}}^{QPCR}(\tau | X_{T+1}) = \sum_{i=1}^n \hat{Q}_{Y_{T+2}}^{QPCR, \mathcal{G}_i}(\tau | X_{\mathcal{G}_i, T+1})$.

Decomposing GaR into the contributions from individual variables also makes it possible

to create easily trackable and comparable summaries of our ML analyses in the form of sector-specific indices. We note that indices constructed in this way enjoy a series of favourable properties: they are targeted to particular quantiles of interest, they are predictive without suffering from look-ahead bias, and they isolate sector-specific effects without capturing unrelated information.

For example, the first panel of Figure 4 shows the contribution of financial variables to the $\tau = 0.05$ quantile of one-period-ahead IP growth,⁵ averaged over three months for smoothness, together with the NFCI for comparison. Similarly to the NFCI, our targeted FCI worsens around the GFC, as well as the Covid-19 pandemic and the subsequent tightening cycle. However, in contrast to the NFCI, our targeted FCI improves between 2016 and 2020, suggesting that loose financial conditions helped decrease downside risks in this period. The second panel shows a similar plot for the contribution of labour-market variables,⁶ together with nonfarm payrolls—a commonly used benchmark to assess real economic activity. Similarly to nonfarm payrolls, the targeted labour market index worsens around the GFC and the Covid-19 pandemic. The third panel shows the targeted housing market index and the Case-Shiller house-price index—a commonly used benchmark to assess the US housing market.⁷ The two series show some cyclical comovement, although there are protracted periods where they are asynchronous.

⁵That is, $\hat{Q}_{Y_{T+2}}^{QPCR, \mathcal{G}_{financial}}(\tau | X_{\mathcal{G}_{financial}, T+1})$, where $\mathcal{G}_{financial}$ contains the indices corresponding to the predictors: AAAFFM, BAA, BAAFFM, BOGMBASE, BUSLOANS, COMPAPFFx, CONSPI, CP3Mx, DTCOLNVHFN, DTCTHFN, FEDFUNDS, GS10, GS5, M2REAL, M2SL, NONBORRES, REALLN, S.P.500, S.P.PE.ratio, T10YFFM, T1YFFM, T5YFFM, TB3MS, TB3SMFFM, TB6SMFFM, TOTRESNS, and VIXCLSx.

⁶The predictors included are: AWHMAN, AWOTMAN, CE16OV, CES0600000007, CES0600000008, CES1021000001, CES2000000008, CLAIMSx, CLF16OV, DMANEMP, HWIU-RATIO, MANEMP, NDMANEMP, PAYEMS, SRVPRD, UNRATE, USCONS, USFIRE, USGOOD, and USWTRADE.

⁷The predictors included are: HOUST, HOUSTMW, HOUSTNE, HOUSTS, HOUSTW, PERMITMW, PERMITNE, PERMITS, and PERMITW.



Figure 4: Targeted indices and commonly-used benchmarks.

Note. All indices are normalized to have zero mean and unit variance.

Figure 5 shows the pairwise correlations of the targeted indices and benchmarks considered in Figure 4. As suggested by the plots in Figure 4, we find that our targeted FCI is most highly correlated with the NFCI, that our targeted labour market index is most highly correlated with payrolls, and that our targeted housing index is most highly correlated with the Case-Shiller house price index. We also find that the NFCI is most strongly correlated with our labour market index, and that it is significantly

correlated with payrolls and the Case-Shiller house price index, suggesting that the NFCI is capturing non-financial information. Taken together, these findings highlight the value of constructing dedicated, sector-specific indices using our proposed approach.

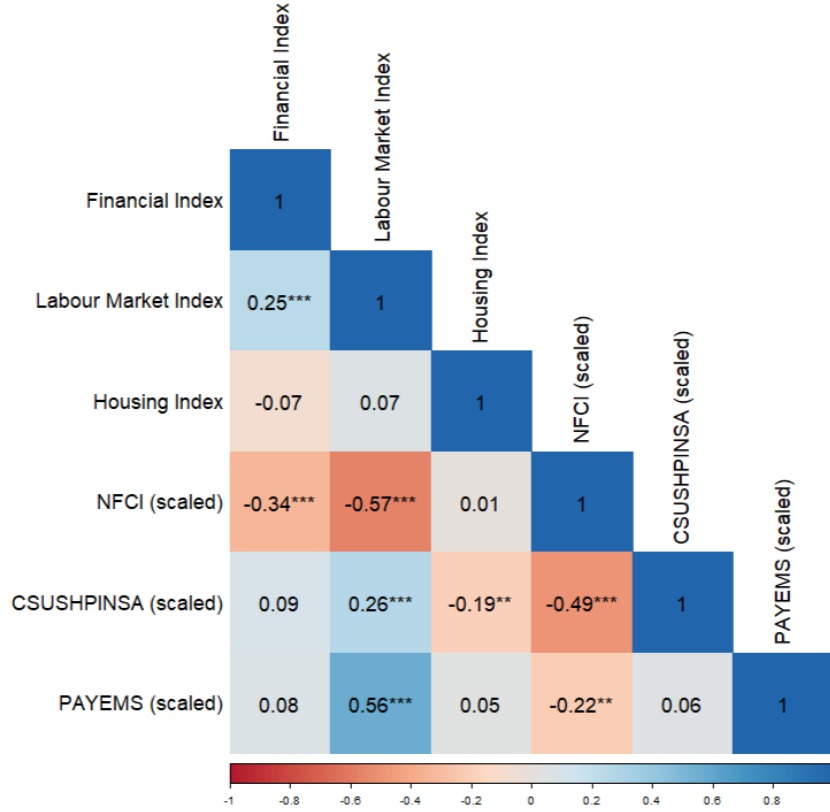


Figure 5: Pairwise correlations of indices and commonly-used benchmarks.

Note. The significance of the correlation between index or benchmark i and j , $r_{i,j}$, is tested under the null hypothesis $H_0 : r_{i,j} = 0$ using the statistic $z = \hat{r}_{i,j} \sqrt{(\tilde{T} - 2)/(1 - \hat{r}_{i,j}^2)}$, where $\hat{r}_{i,j}$ is the sample correlation between i and j and \tilde{T} is the number of observations. *** p -value < 0.01 , ** p -value < 0.05 , * p -value < 0.1 .

5 Conclusion

We applied QPCR to predict downside risk to IP growth, and derived clear insights into growth vulnerabilities. Our analysis showed that financial, labour-market, and housing variables are the primary drivers of risks, with their relative importance evolving over time. Moreover, we validated and quantified commonly held views on key predictors of downside risks, including measures of slack, yield curve dynamics, and credit spreads. We also exploited the linear structure of QPCR to decompose downside risk into variable-by-variable contributions, which allowed us to construct sector-specific indices that are predictive of future vulnerabilities without suffering from look-ahead bias, while adjusting for the information of other sectors. Our framework can be readily adapted to other contexts, offering a flexible toolkit for GaR assessments.

References

- Adrian, M. T., F. Duarte, and T. Iyer (2023). The market price of risk and macro-financial dynamics. *IMF Working Paper* (23/199), 1–87.
- Adrian, T., N. Boyarchenko, and D. Giannone (2019). Vulnerable growth. *American Economic Review* 109(4), 1263–1289.
- Amburgey, A. J. and M. W. McCracken (2023). On the real-time predictive content of financial condition indices for growth. *Journal of Applied Econometrics* 38(2), 137–163.
- Athey, S., J. Tibshirani, S. Wager, et al. (2019). Generalized random forests. *The Annals of Statistics* 47(2), 1148–1178.
- Bañbura, M., D. Giannone, and L. Reichlin (2010). Large bayesian vector auto regressions. *Journal of applied Econometrics* 25(1), 71–92.
- Belloni, A. and V. Chernozhukov (2011). l1-penalized quantile regression in high-dimensional sparse models. *Annal of Statistics*.
- Brave, S. and D. Kelley (2017). Introducing the chicago fed’s new adjusted national financial conditions index. *Chicago Fed Letters* (386).
- Brownlees, C. and A. B. Souza (2021). Backtesting global growth-at-risk. *Journal of Monetary Economics* 118, 312–330.
- Carriero, A., T. E. Clark, and M. Marcellino (2022). Nowcasting tail risk to economic activity at a weekly frequency. *Journal of Applied Econometrics* 37(5), 843–866.
- Carriero, A., T. E. Clark, and M. Marcellino (2024). Specification choices in quantile regression for empirical macroeconomics. *Journal of Applied Econometrics*.
- Chen, H. and J. Lee (2024). Predictive quantile regression with high-dimensional predictors: The variable screening approach. *mimeo*.

- Clark, T. E., F. Huber, G. Koop, M. Marcellino, and M. Pfarrhofer (2023). Tail forecasting with multivariate bayesian additive regression trees. *International Economic Review* 64(3), 979–1022.
- Clark, T. E., F. Huber, G. Koop, M. Marcellino, and M. Pfarrhofer (2024). Investigating growth-at-risk using a multicountry nonparametric quantile factor model. *Journal of Business & Economic Statistics*, 1–16.
- ECB (2019). *Financial Stability Review, May 2019*. European Central Bank.
- Eguren-Martin, F., S. Kösem, G. Maia, and A. Sokol (2024). Targeted financial conditions indices and growth-at-risk. Technical report, Bank of England.
- ESRB (2024). *Improvements to the ESRB macroprudential stance framework*. European Systemic Risk Board.
- Estrella, A. and F. S. Mishkin (1998). Predicting us recessions: Financial variables as leading indicators. *Review of Economics and Statistics* 80(1), 45–61.
- Fan, J. and R. Li (2001). Variable selection via nonconcave penalized likelihood and its oracle properties. *Journal of the American statistical Association* 96(456), 1348–1360.
- Gertler, M. and C. S. Lown (1999). The information in the high-yield bond spread for the business cycle: evidence and some implications. *Oxford Review of economic policy* 15(3), 132–150.
- Giannone, D., M. Lenza, and G. E. Primiceri (2015). Prior selection for vector autoregressions. *Review of Economics and Statistics* 97(2), 436–451.
- Gilchrist, S. and E. Zakrajšek (2012). Credit spreads and business cycle fluctuations. *American economic review* 102(4), 1692–1720.
- IMF (2017). *Global Financial Stability Report, October 2017: Is Growth at Risk?*. International Monetary Fund.

- IMF (2024). *Global Financial Stability Report, October 2024: Macroeconomic Stability and High Global Economic Uncertainty*. International Monetary Fund.
- Kock, A. B., M. Medeiros, and G. Vasconcelos (2020). *Penalized Time Series Regression*, Chapter 7, pp. 193 – 228. Springer.
- Kotchoni, R., M. Leroux, and D. Stevanovic (2019). Macroeconomic forecast accuracy in a data-rich environment. *Journal of Applied Econometrics* 34(7), 1050–1072.
- Lenza, M., I. Moutachaker, and J. Paredes (2023). *Density forecasts of inflation: a quantile regression forest approach*. Number 2830. ECB Working Paper.
- Ma, S., R. Li, and C.-L. Tsai (2017). Variable screening via quantile partial correlation. *Journal of the American Statistical Association* 112(518), 650–663.
- McCracken, M. and S. Ng (2020). Fred-qd: A quarterly database for macroeconomic research. Technical report, National Bureau of Economic Research.
- Medeiros, M. C., G. F. Vasconcelos, Á. Veiga, and E. Zilberman (2021). Forecasting inflation in a data-rich environment: the benefits of machine learning methods. *Journal of Business & Economic Statistics* 39(1), 98–119.
- Meinshausen, N. (2006). Quantile regression forests. *Journal of Machine Learning Research* 7(Jun), 983–999.
- Plagborg-Møller, M., L. Reichlin, G. Ricco, and T. Hasenzagl (2020). When is growth at risk? *Brookings Papers on Economic Activity* 2020(1), 167–229.
- Prüser, J. and F. Huber (2024). Nonlinearities in macroeconomic tail risk through the lens of big data quantile regressions. *Journal of Applied Econometrics* 39(2), 269–291.
- Sun, C. and M. Medeiros (2024). A sorted penalty estimator: Inference for a correlation-robust shrinkage method. *Available at SSRN*.

- Tibshirani, R. (1996). Regression shrinkage and selection via the lasso. *Journal of the Royal Statistical Society Series B: Statistical Methodology* 58(1), 267–288.
- Zhang, C.-H. (2010). Nearly unbiased variable selection under minimax concave penalty. *Annal of Statistics*.

A Appendix

A.1 Description of acronyms in Fred-MD

Table 3: Description of acronyms in FRED-MD

Acronym	Description	Group
RPI	Real Personal Income	1
W875RX1	Real personal income ex transfer receipts	1
DPCERA3M086SBEA	Real personal consumption expenditures	4
CMRMTSPLx	Real Manu. and Trade Industries Sales	4
RETAILx	Retail and Food Services Sales	4
INDPRO	IP Index	1
IPFPNSS	IP: Final Products and Nonindustrial Supplies	1
IPFINAL	IP: Final Products (Market Group)	1
IPCONGD	IP: Consumer Goods	1
IPDCONGD	IP: Durable Consumer Goods	1
IPNCONGD	IP: Nondurable Consumer Goods	1
IPBUSEQ	IP: Business Equipment	1
IPMAT	IP: Materials	1
IPDMAT	IP: Durable Materials	1
IPNMAT	IP: Nondurable Materials	1
IPMANSICS	IP: Manufacturing (SIC)	1
IPB51222s	IP: Residential Utilities	1
IPFUELS	IP: Fuels	1
CUMFNS	Capacity Utilization: Manufacturing	1
HWI	Help-Wanted Index for United States	2
HWIURATIO	Ratio of Help Wanted/No. Unemployed	2
CLF16OV	Civilian Labor Force	2
CE16OV	Civilian Employment	2
UNRATE	Civilian Unemployment Rate	2
UEMPMEAN	Average Duration of Unemployment (Weeks)	2
UEMPLT5	Civilians Unemployed - Less Than 5 Weeks	2
UEMP5TO14	Civilians Unemployed for 5-14 Weeks	2
UEMP15OV	Civilians Unemployed - 15 Weeks & Over	2
UEMP15T26	Civilians Unemployed for 15-26 Weeks	2
UEMP27OV	Civilians Unemployed for 27 Weeks and Over	2
CLAIMSx	Initial Claims	2
PAYEMS	All Employees: Total nonfarm	2

Continued on next page

Table 3 – continued from previous page

Mnemonic	Description	Group
USGOOD	All Employees: Goods-Producing Industries	2
CES1021000001	All Employees: Mining and Logging: Mining	2
USCONS	All Employees: Construction	2
MANEMP	All Employees: Manufacturing	2
DMANEMP	All Employees: Durable goods	2
NDMANEMP	All Employees: Nondurable goods	2
SRVPRD	All Employees: Service-Providing Industries	2
USTPU	All Employees: Trade, Transportation & Utilities	2
USWTRADE	All Employees: Wholesale Trade	2
USTRADE	All Employees: Retail Trade	2
USFIRE	All Employees: Financial Activities	2
USGOVT	All Employees: Government	2
CES0600000007	Avg Weekly Hours : Goods-Producing	2
AWOTMAN	Avg Weekly Overtime Hours : Manufacturing	2
AWHMAN	Avg Weekly Hours : Manufacturing	2
HOUST	Housing Starts: Total New Privately Owned	3
HOUSTNE	Housing Starts, Northeast	3
HOUSTMW	Housing Starts, Midwest	3
HOUSTS	Housing Starts, South	3
HOUSTW	Housing Starts, West	3
PERMIT	New Private Housing Permits (SAAR)	3
PERMITNE	New Private Housing Permits, Northeast (SAAR)	3
PERMITMW	New Private Housing Permits, Midwest (SAAR)	3
PERMITS	New Private Housing Permits, South (SAAR)	3
PERMITW	New Private Housing Permits, West (SAAR)	3
ACOGNO	New Orders for Consumer Goods	4
AMDMNOx	New Orders for Durable Goods	4
ANDENOx	New Orders for Nondefense Capital Goods	4
AMDMUOx	Unfilled Orders for Durable Goods	4
BUSINVx	Total Business Inventories	4
ISRATIOx	Total Business: Inventories to Sales Ratio	4
M1SL	M1 Money Stock	5
M2SL	M2 Money Stock	5
M2REAL	Real M2 Money Stock	5
BOGMBASE	Monetary Base	5
TOTRESNS	Total Reserves of Depository Institutions	5
NONBORRES	Reserves Of Depository Institutions	5
BUSLOANS	Commercial and Industrial Loans	5
REALLN	Real Estate Loans at All Commercial Banks	5
NONREVSL	Total Nonrevolving Credit	5

Continued on next page

Table 3 – continued from previous page

Mnemonic	Description	Group
CONSPI	Nonrevolving consumer credit to Personal Income	5
S.P.500	S&P's Common Stock Price Index: Composite	8
S.P.div.yield	S&P's Composite Common Stock: Dividend Yield	8
S.P.PE.ratio	S&P's Composite Common Stock: Price-Earnings Ratio	8
FEDFUNDS	Effective Federal Funds Rate	6
CP3Mx	3-Month AA Financial Commercial Paper Rate	6
TB3MS	3-Month Treasury Bill:	6
TB6MS	6-Month Treasury Bill:	6
GS1	1-Year Treasury Rate	6
GS5	5-Year Treasury Rate	6
GS10	10-Year Treasury Rate	6
AAA	Moody's Seasoned Aaa Corporate Bond Yield	6
BAA	Moody's Seasoned Baa Corporate Bond Yield	6
COMPAPFFx	3-Month Commercial Paper Minus FEDFUNDS	6
TB3SMFFM	3-Month Treasury C Minus FEDFUNDS	6
TB6SMFFM	6-Month Treasury C Minus FEDFUNDS	6
T1YFFM	1-Year Treasury C Minus FEDFUNDS	6
T5YFFM	5-Year Treasury C Minus FEDFUNDS	6
T10YFFM	10-Year Treasury C Minus FEDFUNDS	6
AAAFFM	Moody's Aaa Corporate Bond Minus FEDFUNDS	6
BAAFFM	Moody's Baa Corporate Bond Minus FEDFUNDS	6
TWEXAFEGSMTHx	Trade Weighted U.S. Dollar Index	6
EXSZUSx	Switzerland / U.S. Foreign Exchange Rate	6
EXJPUSx	Japan / U.S. Foreign Exchange Rate	6
EXUSUKx	U.S. / U.K. Foreign Exchange Rate	6
EXCAUSx	Canada / U.S. Foreign Exchange Rate	6
WPSFD49207	PPI: Finished Goods	7
WPSFD49502	PPI: Finished Consumer Goods	7
WPSID61	PPI: Intermediate Materials	7
WPSID62	PPI: Crude Materials	7
OILPRICEx	Crude Oil, spliced WTI and Cushing	7
PPICMM	PPI: Metals and metal products:	7
CPIAUCSL	CPI : All Items	7
CPIAPPSL	CPI : Apparel	7
CPITRNSL	CPI : Transportation	7
CPIMEDSL	CPI : Medical Care	7
CUSR0000SAC	CPI : Commodities	7
CUSR0000SAD	CPI : Durables	7
CUSR0000SAS	CPI : Services	7
CPIULFSL	CPI : All Items Less Food	7

Continued on next page

Table 3 – continued from previous page

Mnemonic	Description	Group
CUSR0000SA0L2	CPI : All items less shelter	7
CUSR0000SA0L5	CPI : All items less medical care	7
PCEPI	Personal Cons. Expend.: Chain Index	7
DDURRG3M086SBEA	Personal Cons. Exp: Durable goods	7
DNDGRG3M086SBEA	Personal Cons. Exp: Nondurable goods	7
DSERRG3M086SBEA	Personal Cons. Exp: Services	7
CES0600000008	Avg Hourly Earnings : Goods-Producing	2
CES2000000008	Avg Hourly Earnings : Construction	2
CES3000000008	Avg Hourly Earnings : Manufacturing	2
UMCSENTx	Consumer Sentiment Index	4
DTCOLNVHFN	Consumer Motor Vehicle Loans Outstanding	5
DTCTHFN	Total Consumer Loans and Leases Outstanding	5
INVEST	Securities in Bank Credit at All Commercial Banks	5
VIXCLSx	VIX	8
INDPRO.1	INDPRO.1	9
A2P2	1-mo. Nonfinancial commercial paper A2P2/AA credit spread	10
ABCP	1-mo. Asset-backed/Financial commercial paper spread	11
ABSI	Nonmortgage ABS Issuance (Relative to 12-mo. MA)	12
ABSPREAD	BofAML Home Equity ABS/MBS yield spread	11
BAA2	Moody's Baa corporate bond/10-yr Treasury yield spread	10
BDG	Broker-dealer Debit Balances in Margin Accounts	12
BONDGR	New US Corporate Debt Issuance (Relative to 12-mo. MA)	12
CARSPREAD	UM Household Survey: Auto Credit Conditions Good/Bad spread	10
CBCAR	Commercial Bank 48-mo. New Car Loan/2-yr Treasury yield spread	10
CBILL	3-mo. Financial commercial paper/Treasury bill spread	11
CBPER	Commercial Bank 24-mo. Personal Loan/2-yr Treasury yield spread	10
CCDQ	S&P US Bankcard Credit Card: 3-mo. Delinquency Rate	10
CCG	Consumer Credit Outstanding	10
CCINC	S&P US Bankcard Credit Card: Excess Rate Spread	10
CG	Commercial Paper Outstanding	11
CILARGE	FRB Senior Loan Officer Survey: Tightening Standards on Large C&I Loans	10
CISMALL	FRB Senior Loan Officer Survey: Tightening Standards on Small C&I Loans	10
CITA	Commercial Bank C&I Loans/Total Assets	12
CMBS	BofAML 3-5 yr AAA CMBS OAS spread	11

Continued on next page

Table 3 – continued from previous page

Mnemonic	Description	Group
CMBSI	CMBS Issuance (Relative to 12-mo. MA)	12
COMMODLIQ	COMEX Gold/NYMEX WTI Futures Market Depth	12
CONTA	Commercial Bank Consumer Loans/Total Assets	12
CPH	FRB Commercial Property Price Index	12
CPR	Counterparty Risk Index (formerly maintained by Credit Derivatives Research)	11
CRE	FRB Senior Loan Officer Survey: Tightening Standards on CRE Loans	10
CRG	S&P US Bankcard Credit Card: Receivables Outstanding	10
CTABS	ICE BofAML ABS/5-yr Treasury yield spread	11
CTERM	3-mo./1-wk AA Financial commercial paper spread	11
CTF	ICE BofAML Financial/Corporate Credit bond spread	11
CTMBS	ICE BofAML Mortgage Master MBS/10-year Treasury yield spread	11
CWILL	FRB Senior Loan Officer Survey: Willingness to Lend to Consumers	10
D10	10-yr Constant Maturity Treasury yield	12
D2	2-yr Constant Maturity Treasury yield	12
DCOMM	Commercial Bank Total Unused C&I Loan Commitments/Total Assets	12
DNET	Net Notional Value of Credit Derivatives	12
DURSPREAD	UM Household Survey: Durable Goods Credit Conditions Good/Bad spread	10
EQUITYLIQ	CME E-mini S&P Futures Market Depth	12
FAILS	Treasury Repo Delivery Fails Rate	11
FAILSA	Agency Repo Delivery Failures Rate	11
FAILSC	Corporate Securities Repo Delivery Failures Rate	11
FAILSMBS	Agency MBS Repo Delivery Failures Rate	11
FC	Total Assets of Finance Companies/GDP	12
FCORP	Total Assets of Funding Corporations/GDP	12
FFR	Federal Funds Rate	12
FG	Finance Company Owned & Managed Receivables	10
FINS	S&P 500 Financials/S&P 500 Price Index (Relative to 2-yr MA)	12
GSE	Total Agency and GSE Assets/GDP	12
GVL	FDIC Volatile Bank Liabilities	11
HDQBC	NY Fed Consumer Credit Panel: Loan Delinquency Status: Non-current (Percent of Total Balance)	10
HDQBNP	NY Fed Consumer Credit Panel: New Delinquent Loan Balances (Percent of Current Balance)	10

Continued on next page

Table 3 – continued from previous page

Mnemonic	Description	Group
HDQBNRP	NY Fed Consumer Credit Panel: New Seriously Delinquent Loan Balances (Percent of Current Balance)	10
HH	Household debt outstanding/PCE Durables and Residential Investment	12
HOUSSPREAD	UM Household Survey: Mortgage Credit Conditions Good/Bad spread	10
HY	BofAML High Yield/Moody's Baa corporate bond yield spread	10
INS	Total Assets of Insurance Companies/GDP	12
ITA	Fed funds and Reverse Repurchase Agreements/Total Assets of Commercial Banks	12
JINC	30-yr Jumbo/Conforming fixed rate mortgage spread	10
LHY	Markit High Yield (HY) 5-yr Senior CDS Index	10
LIBID	3-mo. Interbank Deposit Spread (OBFR/LIBID-Treasury)	11
LIG	Markit Investment Grade (IG) 5-yr Senior CDS Index	10
LPH	CoreLogic National House Price Index	12
MBONDGR	New State & Local Government Debt Issues (Relative to 12-mo.h MA)	12
MBSI	Total MBS Issuance (Relative to 12-mo. MA)	12
MCAP	S&P 500, NASDAQ, and NYSE Market Capitalization/GDP	12
MDQ	MBA Serious Delinquencies	10
MG	Money Stock: MZM	10
MINC	30-yr Conforming Mortgage/10-yr Treasury yield spread	10
MLIQ10	On-the-run vs. Off-the-run 10-yr Treasury liquidity pre- mium	11
MMF	FMMFPIAN@USECON	11
MSWAP	Bond Market Association Municipal Swap/State & Local Government 20-yr GO bond spread	10
NACMM	NACM Survey of Credit Managers: Credit Manager's Index	10
NCL	Commercial Bank Noncurrent/Total Loans	10
NFC	Nonfinancial business debt outstanding/GDP	12
OEQ	S&P 500, S&P 500 mini, NASDAQ 100, NASDAQ mini Open Interest	12
OINT	3-mo. Eurodollar, 10-yr/3-mo. swap, 2-yr and 10-yr Trea- sury Open Interest	12
PENS	Total Assets of Pension Funds/GDP	12
RATELIQ	CME Eurodollar/CBOT T-Note Futures Market Depth	12
REIT	Total REIT Assets/GDP	12
REPO	Fed Funds/Overnight Treasury Repo rate spread	11
REPOGCF	GCF Treasury/MBS Repo rate spread	11

Continued on next page

Table 3 – continued from previous page

Mnemonic	Description	Group
REPOGR	Repo Market Volume (Repurchases+Reverse Repurchases of primary dealers)	11
RRE	FRB Senior Loan Officer Survey: Tightening Standards on RRE Loans	10
RTA	Commercial Bank Real Estate Loans/Total Assets	12
RTERM	3-mo./1-wk Treasury Repo spread	11
SBD	Total Assets of Broker-dealers/GDP	12
SMALL	NFIB Survey: Credit Harder to Get	10
SPCILARGE	FRB Senior Loan Officer Survey: Increasing spreads on Large C&I Loans	10
SPCISMAILL	FRB Senior Loan Officer Survey: Increasing spreads on Small C&I Loans	10
SPOVX	CBOE Crude Oil Volatility Index, OVX	10
SPR210	10-yr/2-yr Treasury yield spread	11
SPR23M	2-yr/3-mo. Treasury yield spread	11
STA	Commercial Bank Securities in Bank Credit/Total Assets	12
STKGR	New US Corporate Equity Issuance (Relative to 12-mo. MA)	12
STLOC	Federal, state, and local debt outstanding/GDP	12
SWAP10	10-yr Interest Rate Swap/Treasury yield spread	11
SWAP2	2-yr Interest Rate Swap/Treasury yield spread	11
SWAP3M	3-mo. Overnight Indexed Swap (OIS)/Treasury yield spread	11
TABS	Total Assets of ABS issuers/GDP	12
TED	3-mo. LIBOR/CME Term SOFR-Treasury spread	11
TERM	1-yr./1-mo. LIBOR/CME Term SOFR spread	11
USD	Advanced Foreign Economies Trade-weighted US Dollar Value Index	11
VIX	CBOE Market Volatility Index VIX	11
VOL1	1-mo. BofAML Option Volatility Estimate Index	11
VOL3	3-mo. BofAML Swaption Volatility Estimate Index	11
W500	Wilshire 5000 Stock Price Index	12